

Table IV  
 $^{13}\text{C}$   $T_1$  of Aromatic and Methine Carbons in Low  
 Molecular Weight PS Polymers III and IV at 30 °C in ms

type (PS)	ortho, meta	para	methine	$\rho$
III	152	131	133	1.01
IV	143	128	124	0.97

weight, i.e., below or close to 0.85.

The temperature studies on all polymers reported in this work showed that  $T_1$  increased with temperature, implying that higher  $T_1$  values are associated with lower effective correlation times. This fact and the higher  $\rho$  values associated with the undeuterated terminal portions in both the low and high molecular weight selectively deuterated polymers are consistent with a monotonic decrease in  $\tau_{\text{eff}}$  from the central to the terminal portions. This monotonic decrease cannot be limited to a few terminal units since the higher  $\rho$  values are associated with relatively long terminal portions. It is rather surprising that the terminal segments of the high molecular weight PS-II polymer have higher  $\rho$  and  $T_1$  values than the terminal segments of the lower molecular weight polymers of Table IV. A similar fact is revealed by comparing Tables II and III, which show that polymer chains in the lower molecular weight range (17 500–35 000) have shorter  $T_1$  values than terminal chains that are of comparable length but are contained in the high molecular weight PS-II polymer. Since the average methine  $T_1$  of the high molecular weight PS-I polymer remains near the asymptotic value (about 106 ms), the middle segments must have shorter  $T_1$  that balance the increased  $T_1$  of the terminal segments.

It would first appear from the  $T_1$  data that the terminal segments of the higher molecular weight polymers have greater flexibility than in the low molecular weight polymers. However, another and perhaps more reasonable explanation is that the orientational degrees of freedom

of the interior segments of the high molecular weight polymer contribute to the larger  $T_1$  of the terminal segments. The shorter  $T_1$  of the interior segments would still have to be explained in terms of the additional constraints in their motion as the molecular weight increases.

A more definitive interpretation would require measurements of  $T_1$  at more positions along the chain and analysis of the data in terms of a motion model<sup>7-9</sup> that accounts for the internal degrees of freedom. Such studies are being initiated in our laboratory using fractions of selectively deuterated polymers with very narrow molecular weight distributions and making accurate determination of the extent of deuteration in each molecular weight fraction.

**Acknowledgment.** Support of this work was provided by the donors of the Petroleum Research Fund, administered by the American Chemical Society (Grant PRF-13066-AC6), and by the National Science Foundation (Grant ENG 79-13784). The NMR spectra were obtained on a Jeol FX 90 Q NMR spectrometer purchased in part by a grant from the National Science Foundation.

**Registry No.** Polystyrene, 9003-53-6.

## References and Notes

- (1) Heatley, F. *Prog. NMR Spectrosc.* **1979**, *13*, 47.
- (2) Levine, Y. K.; Birdsall, N. J. M.; Lee, A. G.; Metcalfe, J. C.; Roberts, G. C. K. *J. Chem. Phys.* **1974**, *60*, 2890.
- (3) Lyster, J. R., Jr.; McIntyre, H. M.; Torchia, D. A. *Macromolecules* **1974**, *7*, 11.
- (4) Abragam, A. "The Principles of Nuclear Magnetism"; Clarendon Press: Oxford, 1961.
- (5) Baer, M. *J. Polym. Sci., Part A* **1963**, *1*, 2171.
- (6) Morton, M.; Milkovich, R.; McIntyre, D. B.; Bradley, L. J. *J. Polym. Sci., Part A* **1963**, *1*, 443.
- (7) London, R. E.; Avitabile, J. *J. Chem. Phys.* **1976**, *65*, 2443.
- (8) Kuo, W. S.; Jacobus, O. J.; Savitsky, G. B.; Beyerlein, A. L. *J. Chem. Phys.* **1979**, *70*, 1193.
- (9) Seidman, K.; McKenna, J. F.; Emery, S. E.; Savitsky, G. B.; Beyerlein, A. L. *J. Phys. Chem.* **1980**, *84*, 907.

## Effect of Bead Movement Rules on the Relaxation of Cubic Lattice Models of Polymer Chains

Mehmet T. Gurler, Charles C. Crabb, Deborah M. Dahlin, and Jeffrey Kovac\*

Department of Chemistry, University of Tennessee, Knoxville, Tennessee 37996-1600.  
 Received April 30, 1982

**ABSTRACT:** Monte Carlo computer simulations of the relaxation of cubic lattice models of polymer chains have been performed in order to study the effect of the two-bead crankshaft motion on the terminal relaxation time. Chains of lengths 11–59 bonds were studied, with and without excluded volume. In the absence of excluded volume the longest relaxation time of the chain approximately obeys the Rouse scaling law,  $\tau \sim N^2$ . In the presence of excluded volume the scaling exponent is increased slightly to 2.13. These results differ from those obtained previously by Kranbuehl and Verdier. Reasons for this difference are discussed.

## Introduction

The study of the relaxation of cubic lattice models of polymer chains using Monte Carlo techniques was initiated by Verdier and Stockmayer.<sup>1</sup> The technique has been developed and applied to new problems primarily by Verdier and Verdier and Kranbuehl.<sup>2</sup> Probably the most interesting and important aspect of these conceptually and computationally simple simulations is their ability to explore the effects of excluded volume on the relaxation of polymer chains. Since the chain is modeled as a random walk on a cubic lattice, the excluded volume effect is easily

incorporated by studying the self-avoiding walk. Indeed this has been a major focus of the work of Verdier and Verdier and Kranbuehl.<sup>3</sup> The original results of these workers showed a dramatic and surprising effect of excluded volume on the terminal relaxation time of the chain.

The best way to summarize the results of the Monte Carlo studies of lattice models with and without excluded volume is through scaling relations.<sup>4</sup> In the absence of excluded volume the longest relaxation time of the chain ( $\tau$ ) varies with chain length as predicted by the Rouse model;<sup>5</sup> that is

$$\tau \sim N^2 \quad (1)$$

The early results of Verdier and Kranbuehl showed a very different and surprising behavior

$$\tau \sim N^3 \quad (2)$$

The increase of a factor of  $N$  was much larger than had been expected.

Hilhorst and Deutch<sup>6</sup> analyzed the model used by Verdier and Kranbuehl and concluded that the dramatic slowdown of the relaxation of the chain was not due primarily to the long-range excluded volume effect but to the limited number of bead movement rules employed in the simulations. Hilhorst and Deutch showed that the excluded volume constraint imposes local topological restrictions on the chain and that these restrictions cannot be overcome by the "normal bead" movement rule used in the simulations. The basic problem is that the chain develops a series of "local extrema" which cannot pass through each other. This makes the motion of the chain analogous to the random motion of impenetrable particles confined to a line. Such motion has a natural  $N^3$  time scale. Hilhorst and Deutch suggested that the inclusion of a two-bead "crankshaft motion" would overcome the topological restrictions and reveal the true excluded volume effect on the relaxation of the chain.

Verdier and Kranbuehl have made several efforts to include new types of bead movements into their simulations in order to examine the validity of the Hilhorst and Deutch critique. Their original effort<sup>7</sup> did not succeed in removing the topological restrictions as was pointed out by Boots and Deutch.<sup>8</sup> In a more recent paper, Kranbuehl and Verdier<sup>2</sup> have incorporated a number of two-bead motions into their model and studied the behavior of the longest chain relaxation time as a function of chain length. They find that for short chains the relaxation is speeded up considerably, with a scaling exponent only slightly larger than 2. For chains longer than about 30 bonds, however, the behavior is similar to that found in their previous work, with a scaling exponent near 3. They conclude that Hilhorst and Deutch may be correct for short chains but in longer chains new self-entanglement mechanisms come into play that slow down the relaxation.

The results of Kranbuehl and Verdier disagree with several other Monte Carlo studies in which two-bead motions were used.<sup>9,10</sup> They attempt to rationalize this disagreement by pointing out either that only short chains were studied or that the relaxation time was measured by studying the relaxation of highly extended conformations. This method for calculating  $\tau$  had previously been shown to give anomalously short relaxation times compared to those obtained from the equilibrium autocorrelation function. This latter statement has been challenged recently by Heilmann and Rotne.<sup>10</sup>

In light of the disagreement between the various computer studies, the plausibility of the Hilhorst-Deutch analysis and the rather implausible suggestion that qualitatively different mechanisms could be operating for short and long chains, we decided to do a Monte Carlo study of the relaxation of cubic lattice model chains as a function of chain length using a simple 90° crankshaft motion in addition to the normal bead and end-bead motions used in the original Verdier and Stockmayer model. The details of the model are presented and the results are reported in the following sections.

### The Model

The polymer chain is represented as a random walk of  $N - 1$  steps of unit length confined to a cubic lattice. Each

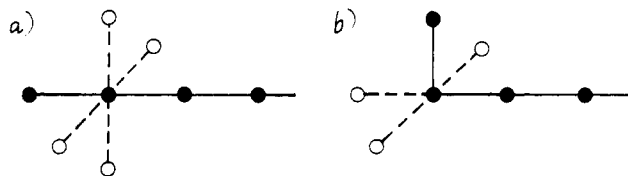


**Figure 1.** Possible end-bead motions. The original chain conformation is indicated by solid lines and filled circles. The possible new conformations are indicated by dashed lines and open circles.



**Figure 2.** Linear conformation. None of the bonds shown can move.

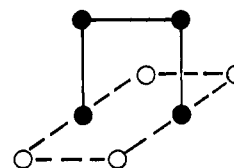


**Figure 3.** Crankshaft motion. The original chain conformation is indicated by solid lines and filled circles. The possible new conformations are indicated by dashed lines and open circles.

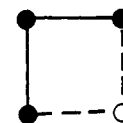


**Figure 4.** Normal bead motion. The original chain conformation is indicated by solid lines and filled circles. The possible new conformation is indicated by dashed lines and an open circle.

of the steps is referred to as a bond. The chain occupies  $N$  lattice junction points. Each of these points is called a bead. The chain is moved according to the following algorithm, which is similar to that used in all studies of the type. The initial description refers to the case where excluded volume is present.

First a bead is chosen at random. If it is an end bead, then one of the 90° motions shown in Figure 1 is attempted. The particular motion attempted is chosen at random with equal probability for each choice. If the potential location of the bead is occupied by another bead, then the move is not made, the bead cycle terminates, and a new bead is chosen.

If the chosen bead is an interior bead, the local conformation around the bead is investigated. Here there are three possibilities, shown in Figures 2-4. In the linear conformation shown in Figure 2 no motions are allowed so the bead cycle is terminated immediately. If the linear conformation is not found, then the conformation is either the crankshaft structure shown in Figure 3 or the bent conformation shown in Figure 4. If the crankshaft structure is present, then a 90° motion is attempted; the direction is chosen at random with equal probability for each direction. This is shown in Figure 3. If the conformation is bent, the normal bead motion shown in Figure 4 is attempted. At this point a bead cycle is completed and a new bead is chosen. Self-reversals of conformation are not prohibited if the same bead is chosen again.

In the absence of excluded volume several modifications must be made since the chain may overlap itself. The end bond in the bent conformation is allowed to flip over onto the chain. When the crankshaft structure is found, a random choice is made between the crankshaft motion and the normal bead motion, with equal probability for the two. If a "degenerate crankshaft" composed to two bonds is located, it is not allowed to move. Of course, no move is excluded because of overlap with the chain. When the

Table I  
Mean Square End-to-End Distance  $\langle R^2 \rangle$  in Lattice Units as a Function of Chain Length with and without Excluded Volume<sup>a</sup>

$N - 1$	$\langle R^2 \rangle$	
	no excluded volume	excluded volume
11	11.104 (0.056)	18.857 (0.109)
23	23.402 (0.441)	46.154 (0.672)
35	36.091 (0.963)	76.180 (2.194)
47	48.795 (1.933)	107.990 (3.162)
59	60.095 (3.335)	140.222 (5.505)

<sup>a</sup> The figures in parentheses are the standard deviations from at least eight runs.

Table II  
Terminal Relaxation Times in Units of  $N$  Bead Cycles as a Function of Chain Length with and without Excluded Volume<sup>a</sup>

$N - 1$	$\tau_0$ (no excluded volume)	$\tau$ (excluded volume)	$\tau/\tau_0$
11	20.2 (0.5)	38.5 (0.9)	1.91
23	78.0 (3.2)	179.3 (7.8)	2.30
35	168.4 (8.1)	441.3 (29.9)	2.62
47	320.4 (39.7)	874.5 (119.6)	2.73
59	465.6 (51.3)	1326.2 (145.3)	2.85

<sup>a</sup> The figures in parentheses are the standard deviations from at least seven runs.

crankshaft motion is included, the relaxation of the chain in the absence of excluded volume seems to be more sensitive to the fine details of the algorithm than we expected from previous work. The model used here seems roughly comparable to that used by Kranbuehl and Verdier<sup>2</sup> and consistent with that used in the excluded volume case.

From time to time the chain conformation is sampled and the end-to-end vector and the center-of-mass coordinates are stored as a function of the number of bead cycles completed. Since the natural time scale of the chain is approximately proportional to  $N$ , the sampling is done each  $10N$  bead cycles. After a total of  $13500N$  bead cycles have been completed, the run is terminated and the data are analyzed.

Following Verdier and Kranbuehl the data are analyzed in terms of the end-to-end vector autocorrelation function defined as

$$\rho(t) = \langle \vec{R}(t) \cdot \vec{R}(0) \rangle / \langle R^2 \rangle \quad (3)$$

where  $\vec{R}(t)$  is the end-to-end vector at a time  $t$  ( $t$  in  $N$  bead cycles, where  $N$  is the number of beads in the chain) and  $\langle \rangle$  represent an ensemble average approximated as a time average. We have also computed the diffusion constant by computing the quantity  $\langle [\vec{R}(t) - \vec{R}(0)]^2 \rangle$  as a function of  $t$ . The diffusion constant  $D$  is then one-sixth the slope of the plot  $\langle [\vec{R}(t) - \vec{R}(0)]^2 \rangle$  vs.  $t$ , where  $t$  is given in units of  $N$  bead cycles.

To ensure that the equilibrium time correlation function is being computed, the initial conformation in each run is taken as the final conformation of a previous run. This

ensures that the chain is in a fully relaxed equilibrium conformation.

## Results

Monte Carlo simulations have been done for chains of lengths 11, 23, 35, 47, and 59 bonds with and without excluded volume. At least four runs at each chain length were done. The equilibrium values of the mean square end-to-end distance  $\langle R^2 \rangle$  are reported in Table I. In the absence of excluded volume the results agree well with the expected value for the random walk:  $\langle R^2 \rangle = (N - 1)l^2$ , with  $l = 1$ . In the presence of excluded volume the values agree well with the Flory exponent:  $\langle R^2 \rangle = a(N - 1)^{6/5}$ , with  $a = 1$  as is usually found in simulations of this type.

Semilogarithmic plots of some typical autocorrelation functions are shown in Figure 5. After an initial rapid decay the plots are quite linear. The terminal relaxation time was estimated by fitting a least-squares line to the linear portions of the curves. These lines are shown in the figures. The negative of the relaxation time  $\tau$  is then the inverse of the slope of the least-squares line. These values are listed in Table II. The time scale used throughout this paper is  $N$  bead cycles. This differs from the time scale used by Kranbuehl and Verdier, who used a time scale of  $N^3$  bead cycles. The values of the relaxation time in the absence of excluded volume are comparable to those obtained in previous work when converted to the same units.

We have taken care to make all runs long enough to produce what appears to be a long limiting linear region of the autocorrelation function. The length of that linear region is at least one complete relaxation time. There is obviously some judgment here, but the results for the relaxation time do not depend significantly on the choice of the linear region as long as the region looks to be linear to the eye and a ruler. The difference in relaxation times resulting from different choices of the linear region is much smaller than the difference in relaxation times between individual runs. We, therefore, believe that our estimates of the terminal relaxation time are consistent and accurate. We plan to check this by resolving the relaxation behavior into Rouse modes and calculating the relaxation of the lowest ones, as was done by Verdier.<sup>11</sup>

In Figure 6 we plot  $\ln \tau$  vs.  $\ln (N - 1)$  for both the nonexcluded volume and excluded volume cases in order to examine the scaling relationship. We have fit a least-squares line to each set of points and determined its slope. In the absence of excluded volume the slope of the line is 1.88. When excluded volume is included, the slope increases slightly to 2.13. We do not see the dramatic change in slope at  $N = 30$  observed by Kranbuehl and Verdier. In Figure 7 we have plotted  $\ln (\tau/\tau_0)$  vs.  $\ln (N - 1)$ , where  $\tau_0$  is the relaxation time in the absence of excluded volume and  $\tau$  is the relaxation time with excluded volume. Here again there is no evidence of a significant change in behavior with increasing chain length.

We have also computed the diffusion constant for the chain, and those results are reported in Table III. They are also plotted in Figure 8 in the form  $\ln (D_0/D)$  vs.  $\ln$

Table III  
Diffusion Constants in Lattice Units Squared per  $N$  Bead Cycles as a Function of Chain Length with and without Excluded Volume<sup>a</sup>

$N - 1$	$D_0$ (no excluded volume)	$D$ (excluded volume)	$D_0/D$
11	0.018 230 (0.001 538)	0.022 644 (0.019 89)	0.805
23	0.011 289 (9.001 092)	0.011 673 (0.001 980)	0.967
35	0.006 963 (0.000 408)	0.007 962 (0.001 380)	0.875
47	0.005 771 (0.000 569)	0.005 545 (0.000 202)	1.041
59	0.004 239 (0.000 768)	0.004 070 (0.000 797)	1.042

<sup>a</sup> The figures in parentheses are the standard deviations from at least four runs.

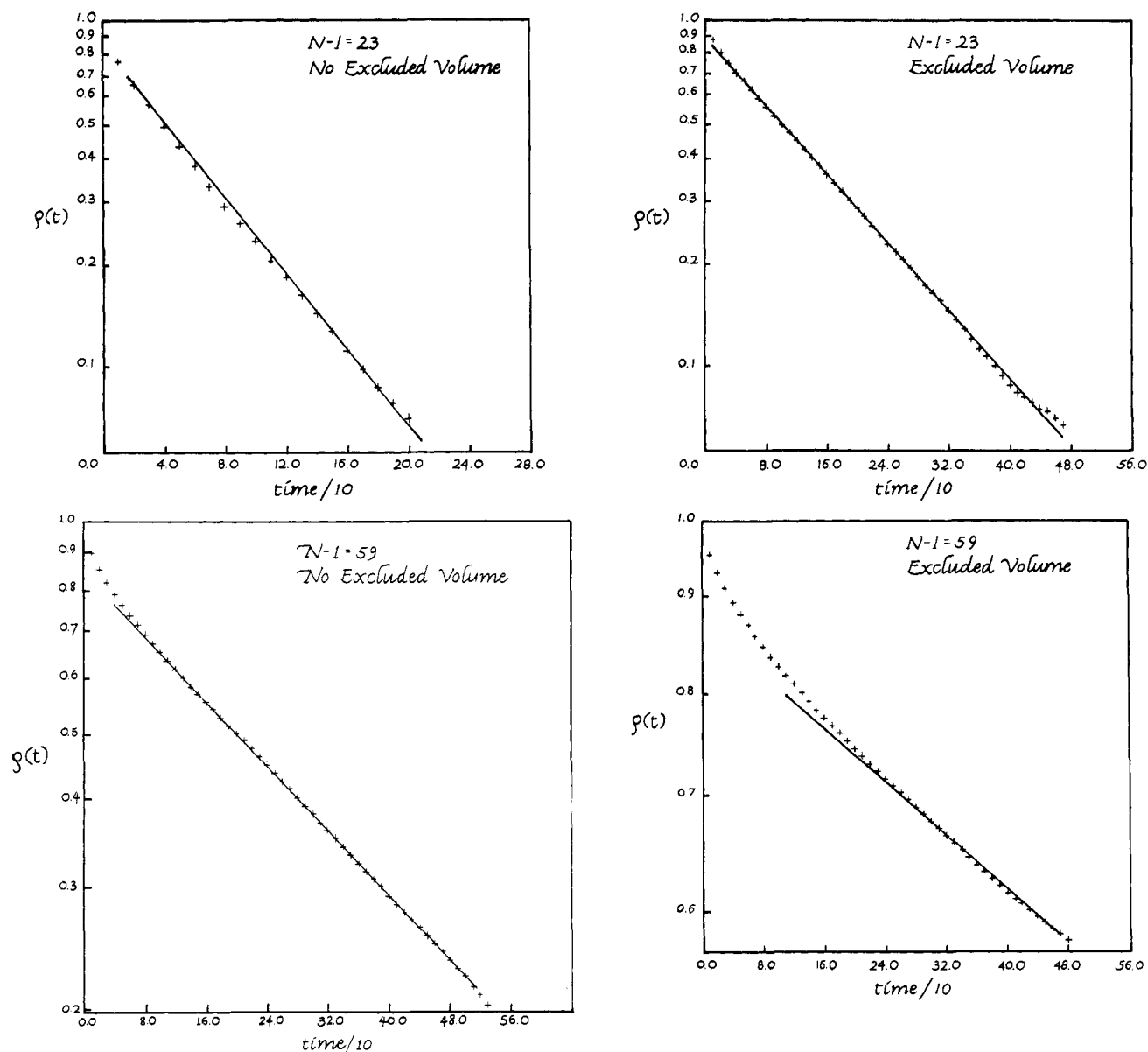


**Figure 5.** Semilogarithmic plots of typical autocorrelation functions  $\rho(t)$  as a function of time ( $t$ ), with  $t$  in  $N$  bead cycles. The solid lines shown are the least-squares lines used to estimate the terminal relaxation times.

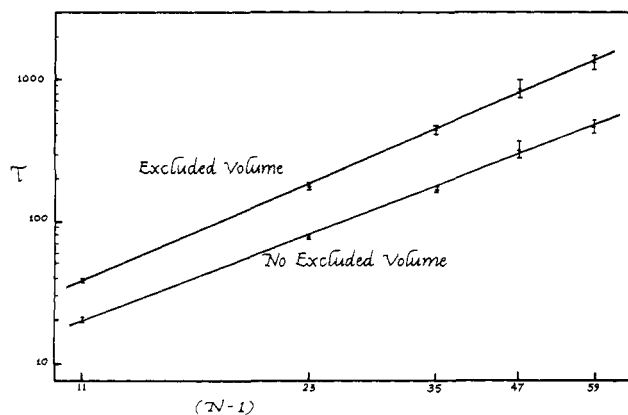


**Figure 6.** Double-logarithmic plot of relaxation time  $\tau$  vs. chain length  $(N-1)$  used to determine scaling exponents. The solid lines are least-squares fits. Both the nonexcluded volume and excluded volume cases are shown.

$(N-1)$ , where  $D_0$  is the diffusion constant in the absence of excluded volume and  $D$  the diffusion constant with excluded volume. The behavior here is similar to that seen for the relaxation times, with no dramatic change in slope

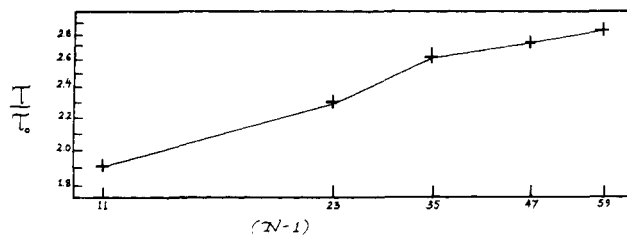


**Figure 7.** Double-logarithmic plots of the ratio of relaxation times  $\tau/\tau_0$ , where  $\tau$  is the relaxation time with excluded volume and  $\tau_0$  the relaxation time without excluded volume, vs. chain length  $(N-1)$ . The lines drawn are only to guide the eye.

as the chain length increases.

### Discussion

The major results of this study are that the inclusion of the  $90^\circ$  crankshaft motion in the simulation algorithm for cubic lattice model chains with excluded volume results in a reduction in the terminal relaxation times relative to those found by Verdier using only the normal bead motion and that this reduction is uniform over the entire range of chain lengths studied. The dramatic change in behavior

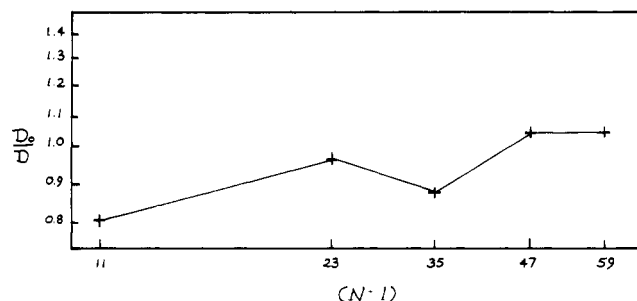


**Figure 8.** Double-logarithmic plot of the ratio of the diffusion constants  $D_0/D$ , where  $D$  is the diffusion constant with excluded volume and  $D_0$  is the diffusion constant without excluded volume, vs. chain length  $(N-1)$ . The lines drawn are only to guide the eye.

at chain lengths near 30 seen by Kranbuehl and Verdier<sup>2</sup> did not occur in our simulation. For chains without excluded volume the behavior of the relaxation time is essentially Rouse-like. The scaling exponents are 1.88 and 2.13 for the nonexcluded volume and excluded volume cases, respectively.

The scaling exponents found in this study are slightly smaller than the Rouse value of 2.0, without excluded volume, and the scaling prediction of 2.2, with excluded volume. The error bars on the estimates of the relaxation times are large enough to encompass the predicted values, particularly if one ignores the point at  $N = 12$ , where it is least likely that long-chain behavior has been attained. There are two other possible sources of error. The first is that the slope of the linear portion of the semilogarithmic plot of the autocorrelation function may not be an accurate estimate of the longest relaxation time. A more accurate estimate would involve the calculation of the autocorrelation function of the normal coordinates as was done by Verdier.<sup>11</sup>

The second problem is end effects. In our model a two-bond motion is not allowed if either the end bead or next to end bead is chosen. This will slow down the chain relaxation and the slowing down will be greater for shorter chains, where the end beads are a relatively large fraction of the total. This slowing down at short chain lengths will decrease the scaling exponent. To investigate this problem it would be necessary to study longer chains. This could be done, but only at the expense of even more computer time. Runs for 59 bonds with excluded volume take nearly 1 h of CPU time on the IBM 370-3031.

The time scale used in this work has been  $N$  bead cycles rather than the  $N^3$  bead cycles used by Kranbuehl and Verdier. We believe that this is the better choice for the following reason. The natural time scale of the chain is actually  $N$  attempted single-bead moves. When the crankshaft is included, the time scale of  $N$  cycles is an overestimate because each bead will have more than one chance to move per time unit. The number of crankshafts per unit chain length ought to be constant so the fractional decrease in the time unit will be the same for all chain lengths at least for long chains. If the  $N^3$  time scale is used, the fraction by which the time scale is shortened will be cubed. This emphasizes this factor and may cause significant deviations at short chain lengths, where the fraction may differ from its long-chain value. The  $N$  bead cycle time scale minimizes the possible effects for short chains and is easier to interpret. We therefore suggest that the  $N$  bead cycle time scale be adopted as the standard choice in simulations of this type.

The results obtained in this paper are consistent with those obtained in some previous studies<sup>9,10</sup> and with the analysis of Hilhorst and Deutch<sup>6</sup> but are qualitatively

different from the results of Kranbuehl and Verdier.<sup>2</sup> The obvious question is: What is the difference in the models that produces this difference in results? We cannot give a definite answer here, though one might come from an analysis similar to those of Hilhorst and Deutch<sup>6</sup> and Boots and Deutch.<sup>8</sup> We can, however, offer some observations and ideas.

The main point of the Hilhorst-Deutch analysis of the lattice model with excluded volume is that when only the normal bead motion is used, local extrema are formed in the chain which cannot cross, thus slowing down the overall chain motion. The 90° crankshaft is the simplest mechanism for removing this restriction. Our simulations show that this motion is effective in removing the restriction at all chain lengths studied and revealing the more subtle effects of excluded volume. Why then do the two-bead motions used by Kranbuehl and Verdier result in such unusual behavior?

Kranbuehl and Verdier use three different two-bead moves. Two of them are equivalent to a series of one-bead moves. This can easily be seen by looking at Figure 1b in their paper. The third move is a 180° crankshaft. By looking at various combinations of motions on paper, one can see that the 180° crankshaft does allow two local extrema to pass each other but much less efficiently (i.e., requiring more moves) than the 90° crankshaft. The other two-bead motions being sequences of one-bead motions are not useful in moving the extrema past each other. They can, however, speed up the movement of extrema along the chain. A possible explanation of the Kranbuehl and Verdier results is that for short chains only a few extrema are present and the two-bead moves speed up the sequential diffusion of extrema to the ends of the chains sufficiently to make the overall chain relaxation rather fast. For long chains, however, there are more local extrema and a longer distance to travel to this mechanism becomes ineffective, and the  $N^3$  time scale returns. This is only a suggestion. Other mechanisms are certainly possible and a more complete analysis is needed.

The results presented here show that the cubic lattice model can be used to study the effects of excluded volume on the relaxation of polymer chains as long as a 90° crankshaft motion is included in the algorithm along with the usual normal bead and end-bead moves. We are currently applying our model to more complicated problems, particularly the motion of polymer chains in a melt.

**Acknowledgment** is made to the donors of the Petroleum Research Fund, administered by the American Chemical Society, for support of this research. Acknowledgment is also made to the National Science Foundation for supporting D.M.D. as an Undergraduate Research Participant during the summer of 1981 and to the Atlantic Richfield Foundation for partial support through the ARCO Young Faculty Grant to the Department of Chemistry at the University of Tennessee. We also thank the University of Tennessee Computer Center for their support and patience.

## References and Notes

- (1) Verdier, P. H.; Stockmayer, W. H. *J. Chem. Phys.* **1962**, *36*, 227.
- (2) Kranbuehl, D. E.; Verdier, P. H. *J. Chem. Phys.* **1979**, *71*, 2662 and references therein.
- (3) Verdier, P. H. *J. Chem. Phys.* **1966**, *43*, 2122. Kranbuehl, D. E.; Verdier, P. H. *Ibid.* **1972**, *56*, 3145. Verdier, P. H. *Ibid.* **1973**, *59*, 6119. Kranbuehl, D. H.; Verdier, P. H. *Ibid.* **1977**, *67*, 361.
- (4) deGennes, P.-G. "Scaling Concepts in Polymer Physics"; Cornell University Press: Ithaca, NY, 1979.
- (5) Rouse, P. E. *J. Chem. Phys.* **1953**, *21*, 1273.

- (6) Hilhorst, H. J.; Deutch, J. M. *J. Chem. Phys.* **1975**, *63*, 5153.
- (7) Verdier, P. H.; Kranbuehl, D. E. *Polym. Prepr., Am. Chem. Soc., Div. Polym. Chem.* **1976**, *17*, 148.
- (8) Boots, H.; Deutch, J. M. *J. Chem. Phys.* **1977**, *67*, 4608.
- (9) Heilman, O. J. *Mater. Fys. Medd. Dan. Vid. Selsk.* **1968**, *37*, 2. Rotne, J.; Heilmann, O. J. Proceedings of the VII International Conference on Rheology, 1976, p 510. Lax, M.; Brender, C. *J. Chem. Phys.* **1977**, *67*, 1785. Birshtein, T. M.; Gridnev, V. N.; Gotlib, Yu. Ya.; Skvortsov, A. M. *Vysokomol. Soedin., Ser. A* **1977**, *19*, 1398.
- (10) Heilmann, O. J.; Rotne, J. *J. Statist. Phys.* **1982**, *27*, 19.
- (11) Verdier, P. H. *J. Chem. Phys.* **1973**, *59*, 6119.

## Multitechnique Solid-State NMR Approach To Assessing Molecular Motion: Poly(butylene terephthalate) and Poly(butylene terephthalate)-Containing Segmented Copolymers. 4

Lynn W. Jelinski\* and Joseph J. Dumais

Bell Laboratories, Murray Hill, New Jersey 07974

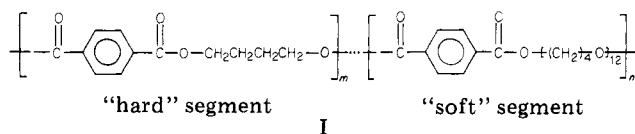
A. K. Engel

E. I. du Pont de Nemours and Company, Polymer Products Department, Wilmington, Delaware 19898. Received August 25, 1982

**ABSTRACT:** Solid-state  $^{13}\text{C}$  NMR has been used to assess the nature of the molecular motions for every carbon of the segmented copolymer poly(butylene terephthalate-co-tetramethyleneundecakis(oxytetramethylene) terephthalate). Relaxation time experiments (see following paper) have been used in conjunction with low-temperature magic-angle spinning (MAS), spinning about an axis displaced from the magic angle, and static powder pattern difference spectroscopy. The results from these experiments (1) confirm that the chemical shift parameters obtained from earlier studies (Jelinski, L. W. *Macromolecules* **1981**, *14*, 1341) are correct, (2) suggest that the aromatic rings undergo  $180^\circ$  ring flips at  $22^\circ\text{C}$  in the copolymer with 0.80 mole fraction hard segments, (3) indicate that the soft-segment ( $\text{CH}_2$ ) carbons exhibit dipolar broadening at temperatures just below their glass transition temperature, and (4) establish that the chemical shift powder pattern line width for the  $-\text{CH}_2\text{CH}_2\text{CH}_2\text{CH}_2-$  carbons of poly(butylene terephthalate) and the segmented copolymers is 17.6 ppm at  $22^\circ\text{C}$ . The advantages and limitations of these solid-state NMR techniques, as they relate to polymers, are discussed in a parallel treatment with the NMR results.

### Introduction

We report here results of a solid-state  $^{13}\text{C}$  NMR study of molecular motion in the segmented copolymer system poly(butylene terephthalate-co-tetramethyleneundecakis(oxytetramethylene) terephthalate) (I). The



poly(butylene terephthalate) “hard” segments and the poly(tetramethyleneundecakis(oxytetramethylene) terephthalate) “soft” segments of this copolymer are not miscible and thus lead to phase separation.<sup>1</sup> However, in contrast to the discrete domain structures found in polystyrene-polybutadiene<sup>2</sup> or polystyrene-polyisoprene,<sup>2</sup> for example, the hard and soft segments in copolyester I are more intimately dispersed. This copolymer thus presents a unique opportunity to study a system in which there is a large interfacial area. Further, the composition of the polymer can be varied by changing the  $m/n$  ratio, which affords an additional experimental variable.

The results presented here, taken together with other data,<sup>3-5</sup> enable us to estimate the nature of the molecular motion in copolymer I. Our goals in this work are to elucidate the molecular motion at each carbon site, to clarify the influences that compositional differences have on these molecular motions, and thus to understand the relationships responsible for the molecular dynamics of this copolymer series.

As a technique for measuring motional frequencies and amplitudes in solids, high-resolution solid-state  $^{13}\text{C}$  NMR

is sensitive to motions spanning the kilohertz to megahertz frequency region. Spin-lattice relaxation and nuclear Overhauser enhancement measurements in the bulk are sensitive to spectral density at megahertz frequencies;<sup>6</sup> dipolar broadening phenomena give information about motions having correlation times of ca.  $10^{-5}$ – $10^{-6}$  s;<sup>7,8</sup> the chemical shift anisotropy<sup>9</sup> and spin-lattice relaxation in the rotating frame<sup>8</sup> give information about mid-kilohertz motions, and broadening caused by motions that occur during the revolution period of the magic-angle spinning rotor reflects low-kilohertz motions.<sup>10</sup> Of these techniques, we shall focus here on the chemical shift anisotropy, as measured by off-axis magic-angle spinning, by low-temperature MAS, and by static powder pattern difference spectroscopy. In addition, we present results obtained by observation of the onset of dipolar broadening in the soft-segment carbons. The advantage and limitations of these techniques, as they relate to polymers, are also discussed.

### Materials and Methods

**Samples.** Poly(butylene terephthalate) was obtained from Eastman Chemical Co., and the poly(butylene terephthalate-co-tetramethyleneundecakis(oxytetramethylene) terephthalate) samples were kind gifts from Mr. J. Hedberg of the du Pont Co. The deuterated segmented copolymers were prepared according to literature methods<sup>11</sup> using either butylene-2,2,3,3- $d_4$  glycol or butylene-1,1,2,2,3,3,4,4- $d_8$  glycol (Merck Isotopes) as the starting material. The purity and composition of all polymers were checked by solution-state  $^{13}\text{C}$  NMR according to previously published procedures.<sup>3</sup> The integrity of the deuterated copolymers was established by solution-state  $^2\text{H}$  NMR.

The polymers for  $^{13}\text{C}$  NMR measurements were quenched from the melt, ground at cryogenic temperatures, and packed into Kel-F sample rotors with a nonhydraulic pellet press. The sample weight